

Convective Heat Transfer and MHD Viscoelastic Nanofluid Flow Induced by a Stretching Sheet

G. C. Shit¹ · R. Haldar¹ · S. K. Ghosh²

Published online: 4 August 2015
© Springer India Pvt. Ltd. 2015

Abstract In this paper we have investigated the viscoelastic nano-fluid flow and heat transfer over a stretching sheet in the presence of magnetic field. The effects of Brownian motion and thermophoresis are taken into account. The flow is governed by the viscoelastic non-Newtonian fluid obeying Walter's liquid B' fluid model. The combined effects of stratifications (thermal and concentration) in the mixed convective flow past over a stretching surface is analyzed. The non-linear boundary layer equations together with the boundary conditions are reduced to a system of coupled non-linear ordinary differential equations by using the similarity transformations. The transformed equations are solved numerically by developing a finite difference scheme along with the Newton's linearization technique. The study shows that the thermal boundary layer thickness appreciably increases with the increasing effects of Brownian motion, thermophoresis and magnetic field strength. However, the viscoelasticity of the nanofluid has reducing effect on thermal boundary layer thickness.

Keywords Nanofluid · Viscoelasticity · Magnetic field · Nusselt number

Introduction

Nano-fluids are basically in the form of dispersing solid nanometer-sized particles in fluids such as water, oil or ethylene glycol. These nanoparticles are typically made of metals, oxides and carbon nanotubes. The nanoparticles are also used for biomedical applications, such as magnetic resonance imaging, photothermal therapy, controlled drug delivery, protein separation, biosensors, DNA detection and immunosensors [1]. The nanofluids are responsible for the increase of thermal conductivity and thereby heat transfer. An innovative technique, which uses a mixture of nanoparticles and base fluid, was first introduced by Choi [2] with

✉ G. C. Shit
gopal_iitkgp@yahoo.co.in

¹ Department of Mathematics, Jadavpur University, Kolkata 700032, India

² Department of Mathematics, Garbeta College, Paschim Medinipur, India

an aim to enhance the heat transfer by means of increasing thermal conductivity of fluids. Later on, Buongiorno [3] explored the reasons behind the enhancement of heat transfer of nanofluids and concluded that Brownian diffusion and thermophoresis are responsible for this enhancement. On the basis of this principle, Kuznetsov and Nield [4] and Nield and Kuznetsova [5] have developed the double diffusive natural convective boundary layer flow of a nanofluid past over a flat plate. Influence of stratification is an important aspect in heat and mass transfer analysis. The formation or deposition of the layers is known as the stratification. This phenomenon occurs due to the change in temperature or concentration, or variations in both, or presence of various fluids. In this regard, Hayat et al. [6, 7] have examined the thermal stratification effects in the mixed convection flow of Maxwell as well as Jeffrey fluid over a stretching surface and provided analytical solution via homotopy analysis method. Malvandi and Ganji [8] investigated the effects of nanoparticle migration on force convective flow of alumina/water nanofluid and heat transfer in a cooled parallel-plate channel in the presence of heat generation. Recently, the study of boundary layer flow of nanofluids over a stretching sheet has become the great interest to the researchers because of various technical processes involved in the production of stretching materials. These materials need either heating or cooling for increasing the quality of final products. Crane [9] first studied the boundary layer flow over a stretching sheet, which moves with a velocity varying linearly with a distance from a fixed point. Gupta and Gupta [10] carried out the heat and mass transfer effects on the boundary layer flow of a viscous fluid over a stretching sheet subject to suction or blowing. Khan and Pop [11] have investigated the steady boundary layer flow and heat transfer in nanofluids over a stretching surface by considering the nanoparticle volume fraction. They observed that the local Nusselt number and local Sherwood number are completely dependent on the effects of Lewis number, Brownian motion number and thermophoresis number. Makinde and Aziz [12] studied the effect of convective boundary layer flow and heat transfer and nanoparticle volume fraction over a stretching surface in nanofluid. Malvandi and Ganji [13] carried out the mixed convective heat transfer of water/alumina nanofluid inside a vertical microchannel by employing modified Buongiorno's model. Further, Malvandi and Ganji [14] numerically investigated the laminar flow and convective heat transfer of alumina/water nanofluid inside a circular microchannel in the presence of a uniform magnetic field.

Hassani et al. [15] carried out analytical solution via HAM for the problem of boundary layer flow of a nanofluid past over a linear stretching sheet. They have only considered the effects of Brownian motion and thermophoresis. At the same time Rana and Bhargava [16] presented numerical solution using variational finite element method for the boundary layer flow and heat transfer of a nanofluid over a nonlinearly stretching sheet. They assumed that the sheet is being stretched as the n th power of the distance from the origin. Malvandi et al. [17] have investigated the steady two-dimensional stagnation point flow and heat transfer of a nanofluid over a porous stretching sheet by taking into account the effects of Brownian motion and thermophoresis diffusion of nanoparticles. In a separate study, Malvandi et al. [18] have also solved the same problem by considering non-linear stretching sheet without porous effect. Loganathan and Vimala [19] dealt with the combined influence of MHD, suction and radiation on the forced convection boundary layer flow of a nanofluid over an exponentially stretching sheet embedded in a thermally stratified medium. However all the above mentioned studies are restricted in the Newtonian fluid model. These studies are not examining the effects of viscoelasticity of the nanofluid as well as the effect of magnetic field. But the study of magneto-hydrodynamic (MHD) flow of an electrically conducting nanofluid is of considerable interest in modern metallurgical and metal-working process lies in the purification of molten metals.

Again the non-newtonian fluids are commonly useful in the process of manufacturing coated sheets, foods, plastic polymers, blood etc. Although several studies [20–23] are avail-

able, who considered different kinds of non-Newtonian fluid models. But these studies are not examined through nanofluid models. However, Cheng [24] studied the free convective heat transfer over a truncated cone embedded in a porous medium saturated by a non-Newtonian power-law nanofluid with constant wall temperature and nanoparticle volume fraction without applying magnetic field. Hedayati and Domiarry [25] and Hedayati et al. [26] studied the effects of nanoparticle migration on different nanofluids by employing the hypothesis that the Brownian motion and the thermophoresis are the only responsible mechanisms for nanoparticle migration. Moreover Goyal and Bhargava [27,28] examined the effect of velocity slip condition on the flow and heat transfer of a non-Newtonian viscoelastic nanofluid over a stretching sheet in the presence of applied magnetic field. But their studies are restricted in the consideration of the effects of viscous dissipation and buoyancy force.

Recently, Bhattacharyya and Layek [29] put forwarded a Newtonian model for the steady boundary layer flow of a nanofluid over a permeable stretching sheet in the presence of magnetic field. They pointed out that magnetic field has significant effect on enhancing heat transfer rate. The other studies [30,31] who have considered the effect of magnetic field on the boundary layer flow of nanofluid but restricted in the consideration of non-Newtonian nanofluid model.

This paper aims to study the viscoelastic nanofluid flow and heat transfer over a linearly stretching sheet in the presence of externally applied magnetic field. The effects of Brownian motion and thermophoretic volume fraction of nanoparticles are taken into account. The problem is solved numerically by using finite difference scheme along with the Newton’s linearization technique. The effects of various values of the non-dimensional parameters are examined on the velocity and thermal boundary layers as well as on the heat transfer rate in terms of Nusselt number.

Flow Analysis

Let us consider the steady two-dimensional boundary-layer flow of an incompressible homogeneous, electrically conducting viscoelastic nanofluid past over an isothermal stretching sheet. The flow is assumed to be in the x -direction, which is taken along the sheet and the y -axis is normal to it. Two equal and opposite forces are introduced along the x -axis, so that the sheet is stretched linearly with a velocity proportional to the distance from the fixed origin. The flow of nanofluid takes place in the region $y > 0$ obeying Walters liquid B' fluid model under the action of an externally applied magnetic field. The magnetic field of uniform strength B_0 is applied perpendicular to the sheet. Since there is no external applied electric field and the assumption of the low magnetic Reynolds number, the induced electric field as well as induced magnetic field have been neglected from the present study. The effects of Brownian motion and the thermophoresis of nanoparticles are incorporated in the present model.

Employing Oberbeck–Boussinesq approximations, the governing equations of conservation of mass, momentum, thermal and nanoparticle volume fraction in the boundary layer are taken as (cf. Nield and Kuznetsov [22] and Kuznetsov and Nield [23])

$$\frac{\partial u}{\partial x} + \frac{\partial v}{\partial y} = 0, \tag{1}$$

$$\begin{aligned} \left(u \frac{\partial u}{\partial x} + v \frac{\partial u}{\partial y} \right) = & \nu_f \frac{\partial^2 u}{\partial y^2} - \frac{k_0}{\rho_f} \left\{ u \frac{\partial^3 u}{\partial x \partial y^2} + v \frac{\partial^3 u}{\partial y^3} - \frac{\partial u}{\partial y} \frac{\partial^2 u}{\partial x \partial y} + \frac{\partial u}{\partial x} \frac{\partial^2 u}{\partial y^2} \right\} \\ & + g\beta_t (T - T_\infty) + g\beta_n (N - N_\infty) - \frac{\sigma B_0^2}{\rho_f} u, \tag{2} \end{aligned}$$

$$\left(u \frac{\partial T}{\partial x} + v \frac{\partial T}{\partial y}\right) = \alpha \frac{\partial^2 T}{\partial y^2} + \frac{(\rho c)_p}{(\rho c)_f} \left[D_B \frac{\partial N}{\partial y} \frac{\partial T}{\partial y} + \left(\frac{D_T}{T_\infty}\right) \left(\frac{\partial T}{\partial y}\right)^2 \right] + \frac{\mu_f}{(\rho c)_f} \left(\frac{\partial u}{\partial y}\right)^2, \quad (3)$$

$$u \frac{\partial N}{\partial x} + v \frac{\partial N}{\partial y} = D_B \frac{\partial^2 N}{\partial y^2} + \left(\frac{D_T}{T_\infty}\right) \frac{\partial^2 T}{\partial y^2}, \quad (4)$$

where u and v are the velocity components in the x - and y -directions respectively, T be the temperature, N the nanoparticle volume fraction, ν_f and ρ_f be the coefficient of kinematics viscosity and density of the base fluid, g be the acceleration due to gravity, k_0 the coefficient of viscoelasticity, β_t and β_n be the thermal expansion coefficient and expansion coefficient of nanoparticle volume fraction, σ the electrical conductivity of the nanofluid, T_∞ and N_∞ be the ambient temperature and nanoparticle volume fraction far away from the sheet, α is the thermal diffusivity, $(\rho c)_p$ the effective heat capacity of nanoparticle, $(\rho c)_f$ the effective heat capacity of the base fluid, D_B is the Brownian diffusion coefficient and D_T is the thermophoresis diffusion coefficient.

The boundary conditions for the present problem are taken as

$$u = U_w = bx, \quad v = 0, \quad T = T_w, \quad N = N_w \quad \text{at } y = 0, \quad (5)$$

and

$$u \rightarrow 0, \quad T \rightarrow T_\infty, \quad N \rightarrow N_\infty \quad \text{as } y \rightarrow \infty, \quad (6)$$

where T_w and N_w be the temperature and nanoparticle volume fraction at the sheet. In the above, U_w be the velocity at the sheet with b (> 0) denotes the constant stretching rate.

Now we express the following non-dimensional variables by defining,

$$\psi = \sqrt{bv_f} x f(\eta); \quad \eta = \sqrt{\frac{b}{v_f}} y; \quad \theta(\eta) = \frac{T - T_\infty}{T_w - T_\infty}; \quad \phi(\eta) = \frac{N - N_\infty}{N_w - N_\infty} \quad (7)$$

where ψ is a dimensional stream function defined by $u = \frac{\partial \psi}{\partial y}$ and $v = -\frac{\partial \psi}{\partial x}$, f is a dimensionless stream function, η be the similarity space variable, θ and ϕ are the dimensionless temperature and nanoparticle volume fraction respectively. Using these dimensionless variables, the velocity components in non-dimensional form can be expressed as

$$u = bx f'(\eta), \quad v = -\sqrt{bv_f} f(\eta).$$

The continuity Eq. (1) is satisfied by u and v automatically.

Substituting the dimensionless variables defined in (7) into the Eqs. (2)–(4) yield

$$f'''' + ff'' - f'^2 - K_1 \left[2f' f''' - ff^{iv} - f'^{i2} \right] + (\lambda_t \theta + \lambda_n \phi) - Mf' = 0, \quad (8)$$

$$\theta'' + Pr(f\theta' + N_b \theta' \phi' + N_t \theta'^2 + Ec f''^2) = 0, \quad (9)$$

$$\phi'' + Le f \phi' + \frac{N_t}{N_b} \theta'' = 0. \quad (10)$$

Similarly, the boundary conditions (5) and (6) reduce to

$$f'(\eta) = 1, \quad f(\eta) = 0, \quad \theta(\eta) = 1, \quad \phi(\eta) = 1 \quad \text{at } \eta = 0, \quad (11)$$

and

$$f'(\eta) \rightarrow 0, \theta(\eta) \rightarrow 0, \phi(\eta) \rightarrow 0 \text{ as } \eta \rightarrow \infty, \tag{12}$$

where primes denotes differentiation with respect to η only.

The dimensionless parameters that appear in Eqs. (8)–(10) are defined as $M = \frac{\sigma B_0^2}{b\rho_f}$ the magnetic parameter, $K_1 = \frac{k_0 b}{\rho_f \nu_f}$ the viscoelastic parameter, $N_t = \frac{(\rho c)_p D_T (T_w - T_\infty)}{(\rho c)_f T_\infty \nu_f}$ the thermophoresis parameter, $N_b = \frac{(\rho c)_p D_B (N_w - N_\infty)}{(\rho c)_f \nu_f}$ the Brownian motion parameter, $P_r = \frac{\nu_f}{\alpha}$ the Prandtl number, $E_c = \frac{U_w^2}{C_p (T_w - T_\infty)}$ the Eckert number, $Le = \frac{\nu_f}{D_B}$ be the Lewis number, $\lambda_t = \frac{Gr_x}{Re_x^2} = \frac{g\beta_t (T_w - T_\infty)}{b^2 x}$ the thermal buoyancy parameter, $\lambda_n = \frac{Gn_x}{Re_x^2} = \frac{g\beta_n (N_w - N_\infty)}{b^2 x}$ the solutal buoyancy parameter, $Gr_x = \frac{g\beta_t (T_w - T_\infty) x^3}{\nu_f^2}$ the local Grashof number, $Gn_x = \frac{g\beta_n (N_w - N_\infty) x^3}{\nu_f^2}$ the local modified Grashof number and $Re_x = \frac{U_w x}{\nu_f}$ be the local Reynolds number.

Since the viscoelastic parameter K_1 is very small, it is therefore, reasonable to seek a solution of the nonlinear Eq. (8) in the form

$$f = f_0(\eta) + K_1 f_1(\eta) + \dots \tag{13}$$

Substituting (13) in (8) and equating the like powers of K_1 , we get

$$f_0''' + f_0 f_0'' - f_0'^2 - M f_0' + \lambda_t \theta + \lambda_n \phi = 0, \tag{14}$$

$$f_1''' + f_0 f_1'' - 2f_0' f_1' - M f_1' + f_1 f_0'' - 2f_0' f_0''' + f_0 f_0' v + f_0'^2 = 0, \tag{15}$$

Using (13), the boundary conditions for f_0 and f_1 can be derived from (11) and (12) as

$$f_0 = 0, f_0' = 1 \text{ at } \eta = 0; f_0' \rightarrow 0, \text{ as } \eta \rightarrow \infty \tag{16}$$

$$f_1 = f_1' = 0 \text{ at } \eta = 0; f_1' \rightarrow 0, \text{ as } \eta \rightarrow \infty. \tag{17}$$

The other important characteristics of the present investigation are the local skin-friction coefficient C_f , the local Nusselt number Nu and the local Sherwood number Sh defined by

$$C_f = \frac{\tau_w}{\mu_f (bx) \sqrt{\frac{b}{\nu_f}}} = [1 - K_1] f''(0),$$

$$\text{where } \tau_w = \left(\frac{\mu_f}{\rho_f} \frac{\partial u}{\partial y} \right)_{y=0} - k_0 \left[u \frac{\partial^2 u}{\partial x \partial y} + v \frac{\partial^2 u}{\partial y^2} + \frac{\partial u}{\partial x} \frac{\partial u}{\partial y} \right]_{y=0}, \tag{18}$$

$$Nu = \frac{q_w}{k \sqrt{\frac{b}{\nu_f}} (T_w - T_\infty)} = -\theta'(0),$$

$$\text{where } q_w = -k \left(\frac{\partial T}{\partial y} \right)_{y=0} = -k \sqrt{\frac{b}{\nu_f}} (T_w - T_\infty) \theta'(0), \tag{19}$$

$$Sh = \frac{n_w}{D_B \sqrt{\frac{b}{\nu_f}} (N_w - N_\infty)} = -\phi'(0),$$

$$\text{where } n_w = -D_B \left(\frac{\partial N}{\partial y} \right)_{y=0} = -D_B \sqrt{\frac{b}{\nu_f}} (N_w - N_\infty) \phi'(0). \tag{20}$$

Numerical Results and Discussion

The system of nonlinear couple differential Eqs. (14) and (15) subject to the boundary conditions (16) and (17) are solved numerically by employing finite difference scheme along with the Newton’s linearization technique (cf. Cebeci and Cousteix [32]). However, the linear coupled ordinary differential Eqs. (9) and (10) using the boundary conditions (11) and (12) for θ and ϕ are solved by using finite difference scheme only. The detail numerical procedures can be found in [20,21,32]. The essential features of this technique is that it is based on a finite difference scheme, which has better stability, simple, accurate and more efficient. Implicit finite difference technique leads to a system which is tri-diagonal and therefore speedy convergence. The numerical computation has been carried out by taking grid size $\Delta\eta = 0.01$. We observed that further decrease in $\Delta\eta$ does not bring about any significant change in the results. This confirms the stability and convergence of the present numerical scheme. In order to examine the flow and heat transfer characteristic of the present

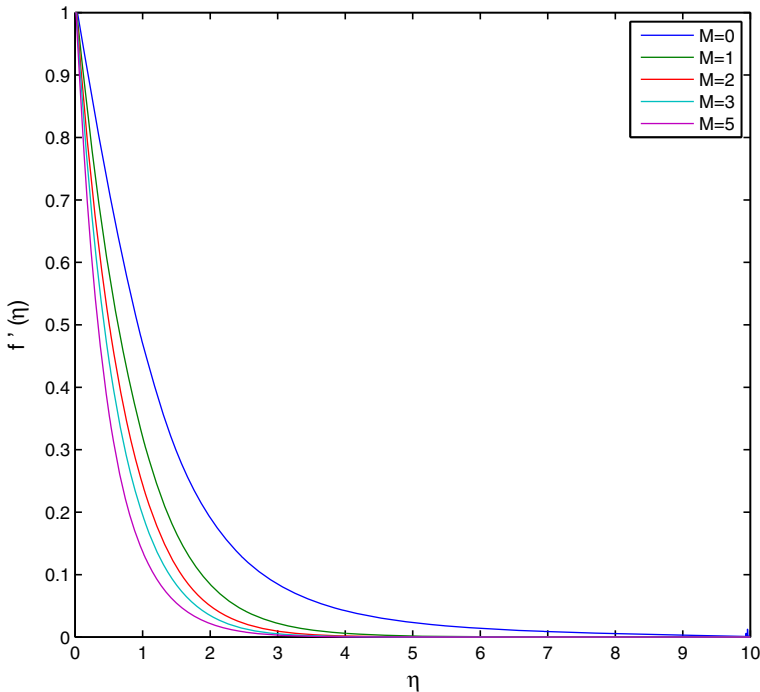


Fig. 1 Variation of $f'(\eta)$ with η for different values of M (when $Pr = 7.0, Nt = 0.3, Nb = 0.5, \gamma = 1.0, \lambda_t = 0.5 = \lambda_n, Ec = 0.002, Le = 10.0, K_1 = 0.01$)

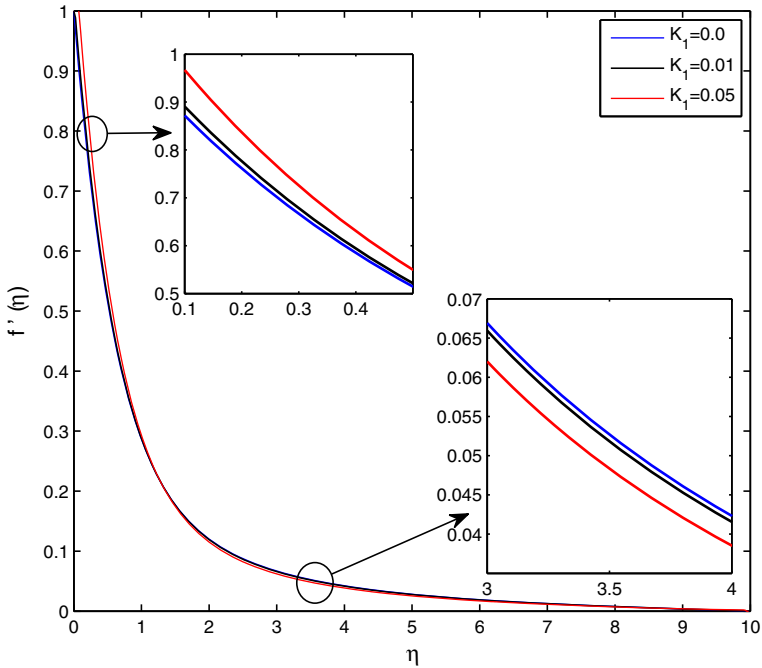


Fig. 2 Variation of $f'(\eta)$ with η for different values of the viscoelastic parameter K_1 (when $M = 2.0, Pr = 7.0, Nt = 0.3, Nb = 0.5, \gamma = 1.0, \lambda_t = 0.5 = \lambda_n, Ec = 0.002, Le = 10.0$)

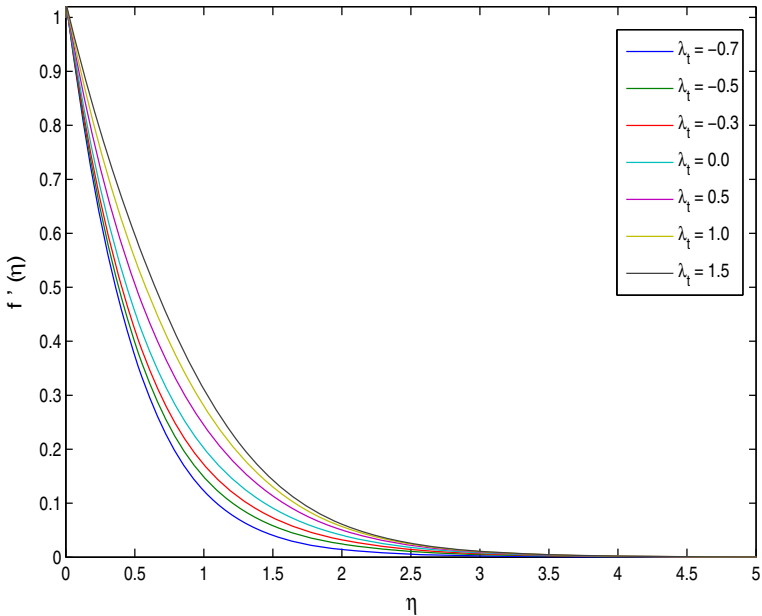


Fig. 3 Variation of $f'(\eta)$ with η for different values of λ_t (when $M = 2.0, Pr = 7.0, Nt = 0.3, Nb = 0.5, \gamma = 1.0, \lambda_n = 0.5, Ec = 0.002, Le = 10.0, K_1 = 0.01$)

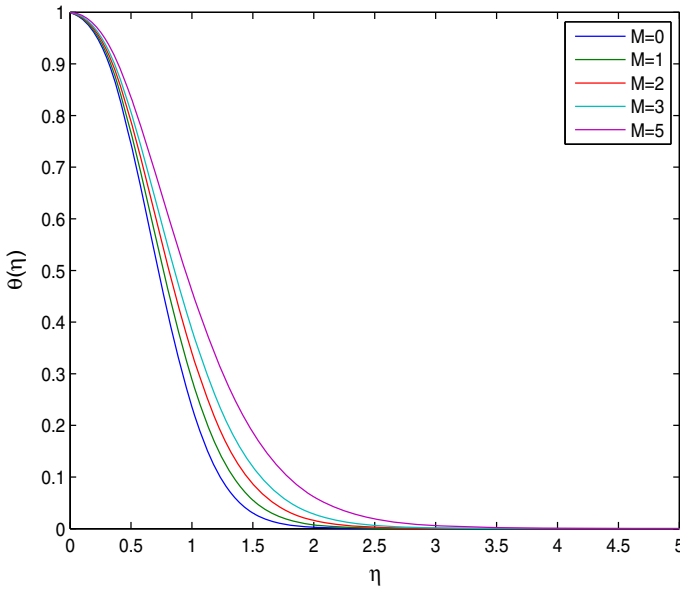


Fig. 4 Distribution of dimensionless temperature $\theta(\eta)$ with η for different values of M (with $Pr = 7.0$, $Nt = 0.3$, $Nb = 0.5$, $\gamma = 1.0$, $\lambda_t = 0.5 = \lambda_n$, $Ec = 0.002$, $Le = 10.0$, $K_1 = 0.01$)

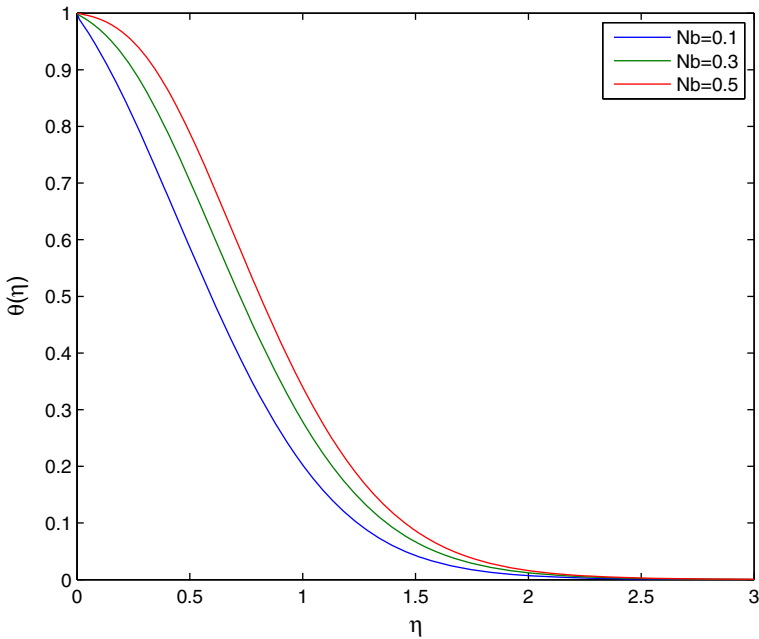


Fig. 5 Distribution of dimensionless temperature $\theta(\eta)$ with η for different values of Nb (when $M = 2.0$, $Pr = 7.0$, $Nt = 0.3$, $K_1 = 0.01$, $\gamma = 1.0$, $\lambda_t = 0.5 = \lambda_n$, $Ec = 0.002$, $Le = 10.0$)

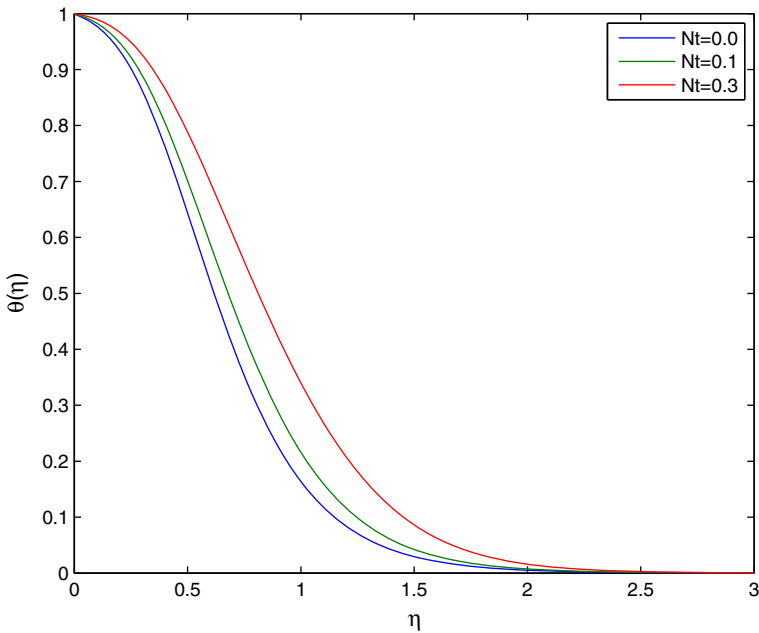


Fig. 6 Distribution of dimensionless temperature $\theta(\eta)$ with η for different values of Nt ($M = 2.0$, $Pr = 7.0$, $Nb = 0.5$, $K_1 = 0.01$, $\gamma = 1.0$, $\lambda_t = 0.5 = \lambda_n$, $Ec = 0.002$, $Le = 10.0$)

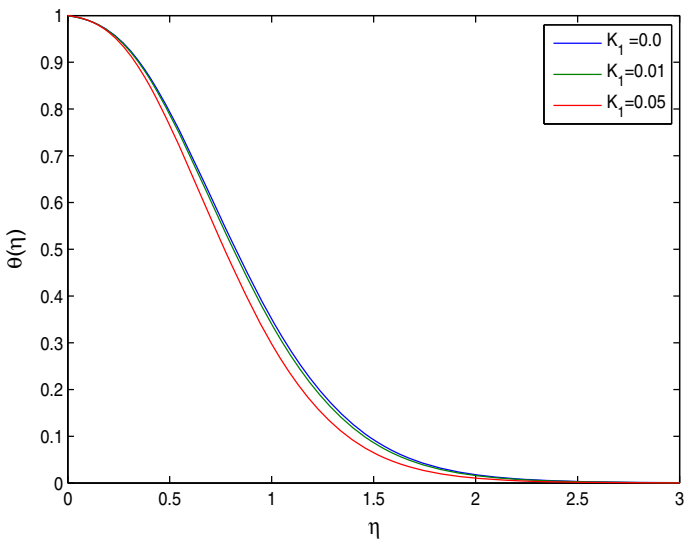


Fig. 7 Distribution of dimensionless temperature $\theta(\eta)$ with η for different values of K_1 (with $M = 2.0$, $Pr = 7.0$, $Nt = 0.3$, $Nb = 0.5$, $\gamma = 1.0$, $\lambda_t = 0.5 = \lambda_n$, $Ec = 0.002$, $Le = 10.0$)

problem, the following values of the different quantities of parameters are invoked in which $0 \leq M \leq 6$, $0 \leq K_1 \leq 0.1$, $0 \leq Nt \leq 1.0$, $5 \leq Le \leq 20$, $-1 \leq \lambda_t \leq 1.5$, $0.1 \leq Nb \leq 0.5$, $-1 \leq \lambda_n \leq 1.5$, $1 \leq Pr \leq 7$.

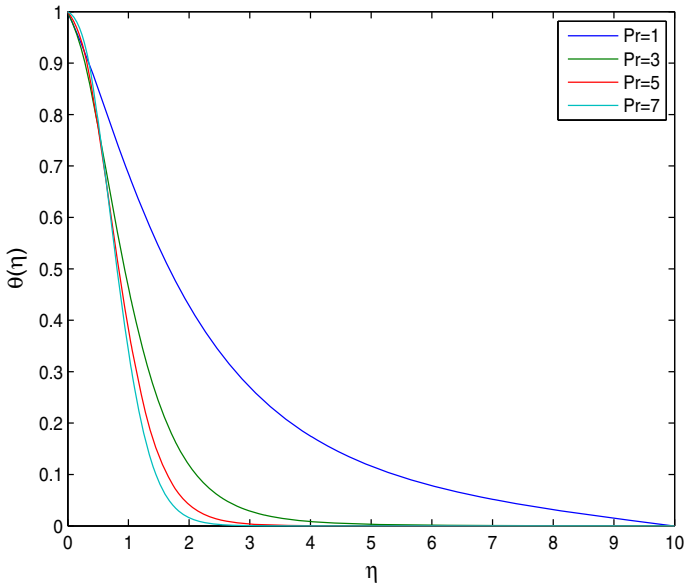


Fig. 8 Distribution of dimensionless temperature $\theta(\eta)$ with η for different values of Pr ($M = 2.0, Nt = 0.3, Nb = 0.5, K_1 = 0.01, \gamma = 1.0, \lambda_t = 0.5 = \lambda_n, Ec = 0.002, Le = 10.0$)

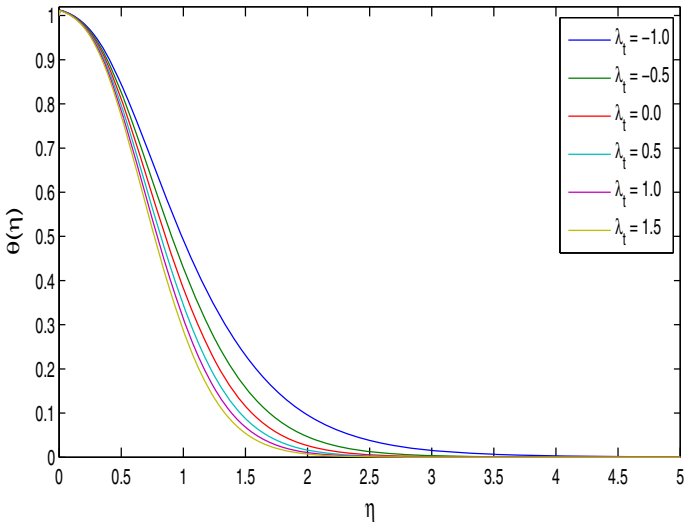


Fig. 9 Distribution of dimensionless temperature $\theta(\eta)$ with η for different values of λ_t (when $M = 2.0, Pr = 7.0, Nb = 0.5, Nt = 0.3, K_1 = 0.01, \gamma = 1.0, \lambda_n = 0.5, Ec = 0.002, Le = 10.0$)

Figures 1, 2 and 3 illustrate the variation of axial velocity along the height from the sheet with different values of the magnetic parameter M , the viscoelastic parameter K_1 and the thermal buoyancy parameter λ_t . Figure 1 shows that the axial velocity gradually decreases with the increase of magnetic parameter M . This happens due to the fact that in the presence of magnetic field there arises a resistive force known as Lorentz force, which

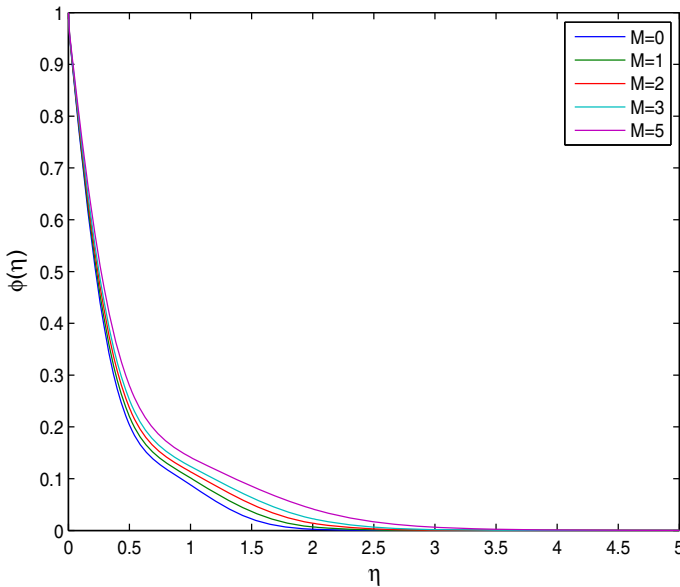


Fig. 10 Variation of nanoparticle volume fraction $\phi(\eta)$ with η for different values of M (with $Pr = 7.0$, $Nt = 0.3$, $Nb = 0.5$, $K_1 = 0.01$, $\gamma = 1.0$, $\lambda_t = 0.5 = \lambda_n$, $Ec = 0.002$, $Le = 10.0$)

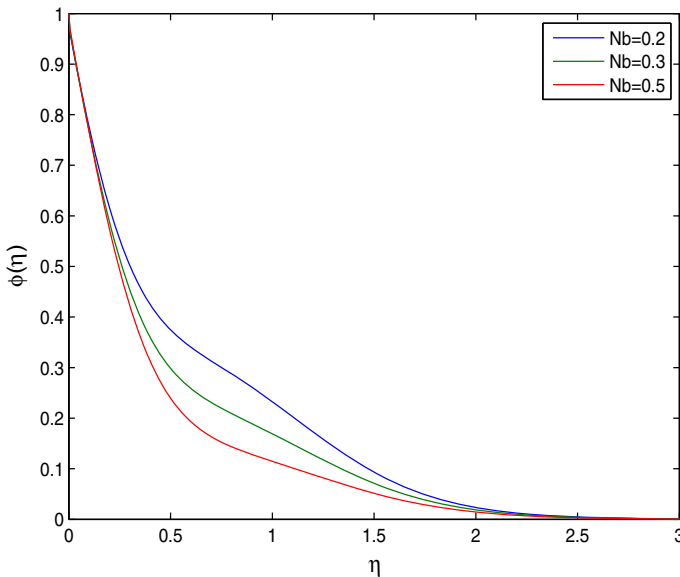


Fig. 11 Variation of nanoparticle volume fraction $\phi(\eta)$ with η for different values of Nb (when $Pr = 7.0$, $K_1 = 0.01$, $Nt = 0.3$, $M = 2.0$, $\gamma = 1.0$, $\lambda_t = 0.5 = \lambda_n$, $Ec = 0.002$, $Le = 10.0$)

has a tendency to slow down the motion of the fluid in the boundary layer. The velocity boundary layer thickness decreases in the presence of strong magnetic field. From Fig. 2 we observe a very interesting result that near the stretching sheet the axial velocity increases with

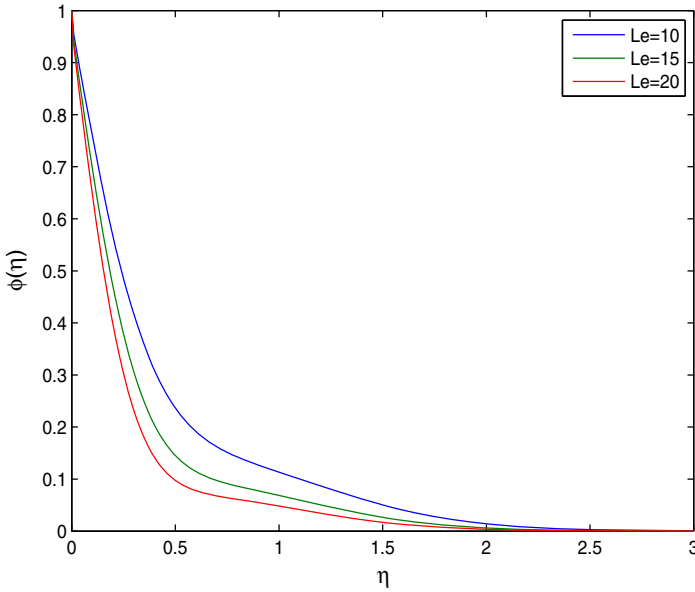


Fig. 12 Variation of nanoparticle volume fraction $\phi(\eta)$ with η for different values of Le (when $Nb = 0.5$, $K_1 = 0.01$, $Nt = 0.3$, $M = 2.0$, $\gamma = 1.0$, $\lambda_t = 0.5 = \lambda_n$, $Ec = 0.002$, $Pr = 7.0$)

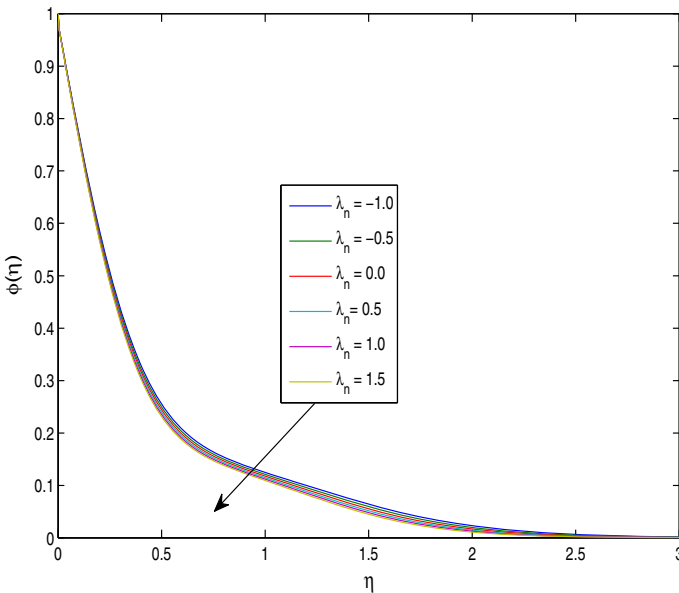


Fig. 13 Variation of nanoparticle volume fraction $\phi(\eta)$ with η for different values of λ_n (with $M = 2.0$, $Pr = 7.0$, $Nt = 0.3$, $Nb = 0.5$, $K_1 = 0.01$, $\gamma = 1.0$, $\lambda_t = 0.5$, $Ec = 0.002$, $Le = 10.0$)

increasing viscoelastic parameter K_1 , while the trend is reverse near the edge of the boundary layer. Therefore, viscoelasticity of the nanofluid play an important role in the boundary layer thickness. It seems that there would be a decrease of boundary layer thickness in the presence

Table 1 The numerical values of the Skin-friction coefficient, Nusselt number and Sherwood number for different physical parameters

Fixed values	Parameters that varying	C_f	$ Nu $	Sh
$Pr = 7, K_1 = 0.01$	$M = 0$	119.7182	0.63202	5.26135
$N_b = 0.5, N_t = 0.3$	$M = 2$	137.2104	0.77514	5.05059
$\lambda_t = \lambda_n = 0.5$	$M = 4$	140.2582	0.828622	4.802206
$Le = 10$	$M = 6$	141.264831	0.864581	4.59237
$Pr = 7, M = 2$	$K_1 = 0.0$	132.28075	0.7515194	4.97113492
$N_b = 0.5, N_t = 0.3$	$K_1 = 0.01$	137.210406	0.7751438	5.0505917
$\lambda_t = \lambda_n = 0.5$	$K_1 = 0.05$	155.759699	0.873585108	5.36750771
$Le = 10$	$K_1 = 0.1$	176.257221	1.00540997	5.76107551
$Pr = 7, K_1 = 0.05$	$N_t = 0.0$	157.196497	0.70503639	4.59806142
$N_b = 0.5, M = 2$	$N_t = 0.2$	156.286321	0.83544107	5.11375114
$\lambda_t = \lambda_n = 0.5$	$N_t = 0.5$	154.574899	0.919942417	5.84681921
$Le = 10$	$N_t = 0.7$	153.232261	0.943300115	6.28795376
$Pr = 7, K_1 = 0.05$	$Le = 5$	152.759505	0.83672963	4.10796308
$N_b = 0.5, N_t = 0.5$	$Le = 10$	154.574899	0.9199424	5.84681921
$\lambda_t = \lambda_n = 0.5$	$Le = 15$	155.210475	0.9320114	7.12008192
$M = 2$	$Le = 20$	155.538012	0.930242647	8.18293968

of thermophoresis parameter and the viscoelasticity of the nanofluid. These results may have greater importance in polymer processing by the choice of the higher order viscoelasticity of the nanofluid to reduce the power consumption. Figure 3 indicates that the axial velocity within the boundary layer has increasing effects on the thermal buoyancy parameter λ_t .

The variation of dimensionless temperature within the boundary layer for different values of the magnetic parameter M , Brownian motion parameter N_b , thermophoresis parameter N_t , viscoelastic parameter K_1 , and Prandtl number Pr are shown in Figs. 4, 5, 6, 7, 8 and 9. Figures 4, 5 and 6 show that the temperature increases significantly with increasing the magnetic parameter, Brownian motion parameter and thermophoresis parameter. These parameters have enhancing effect on the thermal boundary layer thickness due to the presence of nanoparticle in the fluid as well as the applied magnetic field. However, from Figs. 7, 8 and 9 we observe that the temperature has reducing effect for increasing values of the viscoelasticity of the fluid, the Prandtl number Pr and the thermal buoyancy parameter λ_t . Therefore the viscoelastic parameter K_1 , the Prandtl number Pr and the thermal buoyancy parameter λ_t are responsible for increasing thermal boundary layer thickness.

Figures 10, 11, 12 and 13 depict the variation of nanoparticle volume fraction $\phi(\eta)$ along the perpendicular distance from the sheet within the boundary layer. It is interesting to note from Fig. 10 that the volume fraction of nanoparticle increases with increasing magnetic field strength. However, the volume fraction of nanoparticle decreases with increasing the Brownian motion parameter N_b , the Lewis number Le and the solute buoyancy parameter λ_n as shown in Figs. 11, 12 and 13 respectively. Therefore, the presence of magnetic field has enhancing effect on the boundary layer thickness of the nanoparticle volume fraction, while the opposite trend is observed in the case of Brownian motion parameter, the Lewis number and the solute buoyancy parameter.

The important characteristics of the present problem are the skin-friction coefficient (C_f), Nusselt number (Nu) and the Sherwood number (Sh). The mathematical expressions of those physical quantities are presented in the Eqs. (18)–(20) and their corresponding numerical values for various parameters are given in Table 1. From Table 1 we observed that the skin-friction coefficient and the magnitude of the Nusselt number $|Nu|$ increases with increasing magnetic field strength. However, the rate of nanoparticle volume fraction i.e., sherwood number Sh decreases when the magnetic field strength increases. The viscoelasticity of the nanofluid has an enhancing effect on the skin-friction coefficient, the rate of heat transfer $|Nu|$ and the Sherwood number. However, the thermophoresis parameter N_t has a reducing effect on the local skin-friction coefficient C_f , while the parameter N_t has increasing behaviour on the magnitude of the Nusselt number and the Sherwood number. Moreover, the increasing values of the Lewis number Le has an accelerating impact on each of the local skin-friction coefficient and the magnitude of the Nusselt number as well as the rate of nanoparticle volume fraction. This enhancing effect is more significant for Sherwood number.

Concluding Remarks

The effect of viscoelasticity on the nano-fluid flow and heat transfer past over a stretching sheet in the presence of magnetic field has been the main concern in this paper. Moreover the effects of Brownian motion and thermophoretic volume fraction of nanoparticles are taken into account. The governing partial differential equations in the boundary layer have been reduced to a system of couple nonlinear ordinary differential equations under similarity transformation. The transformed governing equations are then solved numerically by using finite difference scheme along with the Newton's linearization technique. From the present analysis the following important findings are summarized as follows.

- The viscoelasticity of the nanofluid has reducing effect on the boundary layer thickness.
- The presence of magnetic field causes decreasing of the velocity boundary layer thickness and enhancement of the thermal boundary layer thickness.
- The thermal buoyancy effect leads to the decreasing of momentum boundary layer thickness and enhancement of the thermal boundary layer thickness.
- The presence of nanoparticle in the viscoelastic fluid increases the thermal boundary layer thickness.
- The volume fraction of the nanoparticle increases with the magnetic field strength.
- The viscoelasticity of the nanofluid has uplifting effect on the local skin-friction, the Nusselt number and the rate of volume fraction of nanoparticle.

Acknowledgments The authors wish to convey their sincere thanks to all the esteemed reviewers for their comments and suggestions based upon which the present version of the manuscript has been revised. One of the authors (G. C. Shit) is thankful to the Institute of Mathematical Sciences, Chennai for providing sufficient research facility to carried out this investigation during his stay at IMSc., Chennai as Visiting Associate.

References

1. Sergei, V.S., Yan, A.I., Sergei, P.K., Mark, S.V., Natalia, V.S., Alexander, G.S., Natalya, L.K., Yury, I.G., Nina, V.C., Elena, K.B., Alexander, G.M.: Recent advances in the synthesis of $Fe_3O_4@AU$ core/shell nanoparticles. *J. Magn. Magn. Mater.* **394**, 173–178 (2015)
2. Choi, S.U.S.: Enhancing thermal conductivity of fluids with nanoparticles. *ASME Fluids Eng. Div.* **231**, 99–105 (1995)

3. Boungiorno, J.: Convective transport in nanofluids. *J. Heat Transf.* **128**, 240–250 (2006)
4. Kuznetsov, A.V., Nield, D.A.: Natural convective boundary-layer flow of a nanofluid past a vertical plate. *Int. J. Therm. Sci.* **49**(2), 243–247 (2010)
5. Nield, D.A., Kuznetsov, A.V.: The Cheng–Minkowycz problem for natural convective boundary-layer flow in a porous medium saturated by a nanofluid. *Int. J. Heat Mass Transf.* **52**(25–26), 5792–5795 (2009)
6. Hayat, T., Shehzad, S.A., Al-Sulami, H.H., Asghar, S.: Influence of thermal stratification on the radiative flow of Maxwell fluid. *J. Braz. Soc. Mech. Sci. Eng.* **35**, 381–389 (2013)
7. Hayat, T., Hussian, T., Shehzad, S.A., Alsaedi, A.: Thermal and concentration stratifications effects in radiative flow of Jeffrey fluid over a stretching sheet. *PLoS One* **9**(10), e107858 (2014)
8. Malvandi, A., Ganji, D.D.: Effects of nanoparticle migration on force convection of alumina/water nanofluid in a cooled parallel-plate channel. *Adv. Powder Technol.* **25**, 1369–1375 (2014)
9. Crane, L.J.: Flow past a stretching plate. *J. Appl. Math. Phys.* **21**(4), 645–647 (1970)
10. Gupta, P.S., Gupta, A.S.: Heat and mass transfer on a stretching sheet with suction or blowing. *Can. J. Chem. Eng.* **55**, 744–746 (1977)
11. Khan, W.A., Pop, I.: Boundary-layer flow of a nanofluid past a stretching sheet. *Int. J. Heat Mass Transf.* **53**, 2477–2483 (2010)
12. Makinde, O.D., Aziz, A.: Boundary layer flow of a nanofluid past a stretching sheet with a convective boundary condition. *Int. J. Therm. Sci.* **50**, 1326–1332 (2011)
13. Malvandi, A., Ganji, D.D.: Mixed convective heat transfer of water/alumina nanofluid inside a vertical microchannel. *Powder Technol.* **263**, 37–44 (2014)
14. Malvandi, A., Ganji, D.D.: Brownian motion and thermophoresis effects on slip flow of alumina/water nanofluid inside a circular microchannel in the presence of a magnetic field. *Int. J. Therm. Sci.* **84**, 196–206 (2014)
15. Hassani, M., Mohammad Tabar, M., Nemati, H., Domairry, G., Noori, F.: An analytical solution for boundary layer flow of a nanofluid past a stretching sheet. *Int. J. Therm. Sci.* **50**, 2256–2263 (2011)
16. Rana, P., Bhargava, R.: Flow and heat transfer of a nanofluid over a nonlinearly stretching sheet: a numerical study. *Commun. Nonlinear Sci. Numer. Simul.* **17**, 212–226 (2012)
17. Malvandi, A., Hedayati, F., Nobari, M.R.H.: An HAM analysis of stagnation-point flow of a nanofluid over a porous stretching sheet with heat generation. *J. Appl. Fluid Mech.* **7**(1), 135–145 (2014)
18. Malvandi, A., Hedayati, F., Nobari, M.R.H.: An analytical study on boundary layer flow and heat transfer of nanofluid induced by a non-linearly stretching sheet. *J. Appl. Fluid Mech.* **7**(2), 375–384 (2014)
19. Loganathan, P., Vimala, C.: MHD flow of nanofluids over an exponentially stretching sheet embedded in a stratified medium with suction and radiation effects. *J. Appl. Fluid Mech.* **8**(1), 85–93 (2015)
20. Shit, G.C., Haldar, R., Sinha, A.: Unsteady flow and heat transfer of a MHD micropolar fluid over a porous stretching sheet in the presence of thermal radiation. *J. Mech.* **29**(3), 559–568 (2013)
21. Shit, G.C., Haldar, R.: Thermal radiation effects on MHD viscoelastic fluid flow over a stretching sheet with variable viscosity. *Int. J. Appl. Math. Mech.* **8**, 14–36 (2012)
22. Shit, G.C., Haldar, R.: Combined effects of thermal radiation and Hall current on MHD free-convective flow and mass transfer over a stretching sheet with variable viscosity. *J. Appl. Fluid Mech.* **5**(2), 113–121 (2012)
23. Prasad, K.V., Pal, D., Umesh, V., Rao, N.S.P.: The effect of variable viscosity on MHD viscoelastic fluid flow and heat transfer over a stretching sheet. *Commun. Non-linear Sci. Numer. Simul.* **15**, 331–344 (2010)
24. Cheng, C.Y.: Free convection of non-Newtonian nanofluids about a vertical truncated cone in a porous medium. *Int. Commun. Heat Mass Transf.* **39**, 1348–1353 (2012)
25. Hedayati, F., Domiarry, G.: Effects of nanoparticle migration and asymmetric heating on mixed convection of $\text{TiO}_2\text{H}_2\text{O}$ nanofluid inside a vertical microchannel. *Powder Technol.* **272**, 250–259 (2015)
26. Hedayati, F., Malvandi, A., Kaffash, M.H., Ganji, D.D.: Mixed convective heat transfer of water/alumina nanofluid inside a vertical microchannel. *Powder Technol.* **269**, 520–531 (2015)
27. Goyal, M., Bhargava, R.: Numerical solution of MHD viscoelastic nanofluid flow over a stretching sheet with partial slip and heat source/sink. *ISRN Nanotechnol.* **2013** (Article ID 931021)(2013)
28. Bhargava, R., Goyal, M.: MHD non-Newtonian nanofluid flow over a permeable stretching sheet with heat generation and velocity slip. *Int. J. Math. Comput. Nat. Phys. Eng.* **8**(6), 910–916 (2014)
29. Bhattacharyya, K., Layek, G.C.: Magnetohydrodynamic boundary layer flow of nanofluid over an exponentially stretching permeable sheet. *Phys. Res. Int.* **2014** (Article Id:592536) (2014)
30. Hamad, M.A.A., Pop, I., Ismail, AImD: Magnetic field effects on free convection flow of a nanofluid past a vertical semi-infinite flat plate. *Nonlinear Anal. Real World Appl.* **12**, 1338–1346 (2011)

31. Ferdows, M., Khan, MdS, Alam, MdM, Sun, S.: MHD mixed convective boundary layer flow of a nanofluid through a porous medium due to an exponentially stretching sheet. *Math. Probl. Eng.* **2012** (Article ID 408528) (2012)
32. Cebeci, T., Cousteix, J.: *Modeling and Computation of Boundary-Layer Flows*. Springer, Berlin (1999)